Wnt Signaling and a Hox Protein Cooperatively Regulate PSA-3/Meis to Determine Daughter Cell Fate after Asymmetric Cell Division in *C. elegans*

Yukinobu Arata,[1] Hiroko Kouike,[2,3,4,8]
Yanping Zhang,[5,9] Michael A. Herman,[5]
Hideyuki Okano,[2,3,4] and Hitoshi Sawa[1,4,6,7,*]
[1] Laboratory for Cell Fate Decision
RIKEN
Center for Developmental Biology
Kobe 650-0047
Japan
[2] Core Research for Evolutional Science and Technology
Japan Science and Technology Corporation
Saitama 332-0012
Japan
[3] Department of Physiology
Keio University School of Medicine
Tokyo 160-8582
Japan
[4] Division of Neuroanatomy
Osaka University Graduate School of Medicine
Osaka 565-0871
Japan
[5] Program in Molecular, Cellular, and Developmental
    Biology
Division of Biology
Kansas State University
Manhattan, Kansas 66506
[6] Division of Bioinformation
Department of Biosystems Science
Graduate School of Science and Technology
Kobe University
Kobe 650-0017
Japan
[7] Precursory Research for Embryonic Science and
    Technology
Japan Science and Technology Corporation
Saitama 332-0012
Japan

Summary

Asymmetric cell division is a mechanism for achieving cellular diversity. In *C. elegans*, many asymmetric cell divisions are controlled by the Wnt-MAPK pathway through POP-1/TCF. It is poorly understood, however, how POP-1 determines the specific fates of daughter cells. We found that *nob-1*/Hox, *ceh-20*/Pbx, and a Meis-related gene, *psa-3*, are required for asymmetric division of the T hypodermal cell. *psa-3* expression was asymmetric between the T cell daughters, and it was regulated by POP-1 through a POP-1 binding site in the *psa-3* gene. *psa-3* expression was also regulated by NOB-1 and CEH-20 through a NOB-1 binding sequence in a *psa-3* intron. PSA-3 can bind CEH-20 and function after the T cell division to promote the proper fate of the daughter cell. These results indicate that cooperation between Wnt signaling and a Hox protein functions to determine the specific fate of a daughter cell.

Introduction

During animal development, a zygote generates diverse cell types that have different temporal and spatial identities; asymmetric cell division is a fundamental mechanism for generating this diversity. In *Drosophila*, the asymmetric divisions of a number of neuroblasts are regulated by the asymmetric segregation of the Numb and Prospero proteins (Jan and Jan, 2001). In *C. elegans*, as described below, many asymmetric divisions are regulated by the Wnt-MAPK pathway. Although the respective mechanisms in each of these organisms are used repeatedly during development, the fates of the daughter cells are distinct and depend on their position in the animal's body. In *Drosophila*, segmentation genes determine the specificities of neuroblast and postmitotic neurons (Bhat, 1999), and, in *C. elegans*, a *Hox* gene, *mab-5*, is involved in cell fate specification after the asymmetric division (Salser and Kenyon, 1996). Therefore, these genes, which regulate positional identity, are likely to be important for determining specificities of cell fates after asymmetric division.

In *C. elegans*, many asymmetric divisions in embryonic and postembryonic development are regulated by the Wnt-MAPK signaling pathway (Herman, 2002; Thorpe et al., 2000). This pathway regulates the asymmetric nuclear localization of the POP-1/TCF transcription factor between daughter cells (POP-1 asymmetry). POP-1 asymmetry is suggested to create distinct POP-1 transcriptional activities in each daughter cell (Kidd et al., 2005; Shetty et al., 2005). POP-1 asymmetry is observed in most cell divisions along the anteroposterior axis (Herman, 2001; Lin et al., 1998). In addition, LIT-1/NLK, a MAP kinase that regulates POP-1 asymmetry, is required for many embryonic and postembryonic divisions (Kaletta et al., 1997; Takeshita and Sawa, 2005). Taken together, these findings indicate that POP-1 functions as a universal factor to determine asymmetry between daughter cells throughout *C. elegans* development. However, in spite of this common mechanism for asymmetric division, the daughter cells have unique cell fates. Therefore, how POP-1 cooperates with genes that regulate positional identity is a critical issue.

Six *Hox* genes are encoded in a loosely linked cluster in *C. elegans*: *ceh-13*, *lin-39*, *mab-5*, *egl-5*, *php-3*, and *nob-1* (Kenyon et al., 1997; Van Auken et al., 2000). Of these, *lin-39*, *mab-5*, and *egl-5* are expressed in a position-specific manner and regulate cell identities (Kenyon et al., 1997). *nob-1* mutants show abnormal tail morphogenesis and the anterior transformation of posterior gut and neural cells, suggesting that *nob-1* regulates positional identity in the posterior region (Van Auken et al., 2000). In many organisms, members of the Pbx and

Meis protein families help the Hox proteins select the correct DNA binding site and regulate their transactivation activity as their cofactors (Mann and Affolter, 1998). The nuclear localization of the Pbx proteins is regulated by their binding with Meis proteins (Affolter et al., 1999). In *C. elegans*, the CEH-20 protein also functions cooperatively with the LIN-39 protein on the promoter of the *hlh-8* and *egl-18* genes to regulate their expression (Koh et al., 2002; Liu and Fire, 2000), suggesting that Hox proteins and their cofactors cooperatively determine spatial specificities in *C. elegans*.

Seam cells, on the lateral sides of the animals, divide asymmetrically in postembryonic development. Among the seam cells, asymmetric division of the T cell is regulated by the Wnt-MAPK signaling pathway, including LIN-44/Wnt, LIN-17/Frizzled, LIT-1, WRM-1/β-catenin, and POP-1 (Herman, 2002; Takeshita and Sawa, 2005). The T cell divides asymmetrically; thus, the anterior daughter (T.a) produces hypodermal cells, while the posterior daughter (T.p) generates neural cells, including the phasmid socket cells. In *pop-1* mutants, the T cell division is symmetric, and both T.a and T.p produce hypodermal cells (Herman, 2001), resulting in the absence of phasmid socket cells (Psa phenotype, for phasmid socket absent). Here, we show that *nob-1/* Hox *ceh-20/*Pbx and a novel Meis-related gene, *psa-3*, are required for the asymmetric T cell division. We found that *psa-3* is expressed asymmetrically between the T cell daughters and that the asymmetric *psa-3* expression is regulated by the Wnt-MAPK pathway as well as by NOB-1 and CEH-20. These findings indicate that two classes of genes, which discretely regulate asymmetric division and positional identity, specify the daughter fates in the asymmetric T cell division.

Results

*psa-3/*Meis, *ceh-20/*Pbx, and *nob-1/*Hox Are Required for the Asymmetric T Cell Division

We identified mutants of *psa-3(os8)*, *ceh-20*, and *nob-1* in a screen for mutants with the Psa phenotype (Sawa et al., 2000), and *psa-3(mh32)* and *psa-3(mh55)* in a screen for phasmid-defective mutants, by using the dye-filling assay (Zhao et al., 2002) (Table 1). The previously identified *ceh-20(ay38)* and *nob-1(ct230)* mutants (Van Auken et al., 2000, 2002) also show the Psa phenotype (Table 1). We determined the T cell lineage in these mutants. In *nob-1*, *ceh-20*, and *psa-3* mutants, the asymmetry of the divisions was often disrupted, leading to the production of hypodermal instead of neural cells by T.p (Figure 1; types II, III, and IV). Therefore, we concluded that these mutants were defective in the asymmetric T cell division. We also observed that the T cell did not divide during the L1 stage in some *nob-1* mutants (Figure 1; type V). In these animals, the nucleus of the T cell was smaller than in wild-type, although the morphology of the nucleus was hypodermal (data not shown), suggesting that the T cell lost its identity in some of the *nob-1* mutants. Such abnormal morphology of the T cell was not observed in other *nob-1* animals or in *ceh-20* or *psa-3* animals.

In *Drosophila* neuroblasts, the Hox genes *abd-A and Abd-B* repress the establishment of cell polarity before division, resulting in the symmetric division of a neuro-

Table 1. *psa-3*, *ceh-20*, and *nob-1* Are Required for Asymmetric T Cell Division

Genotype	% Psa (n)
N2	0% (162)
psa-3(os8)	38.5% (156)
psa-3(os8)[a]	40.0% (60)
psa-3(os8);osEx[pPS3.16]	4.5% (110)
*psa-3(os8);unc-76;osEx[hsp::*PSA-3*]*[a]	3.1% (126)
*psa-3(os8);unc-76;osEx[hsp::*PSA-3::GFP*]*[a]	4.5% (110)
psa-3(RNAi)	7.0% (242)
psa-3(mh32)	45.8% (120)
psa-3(mh55);him-5	26.9% (120)
psa-3(tm656)	0% (102)
psa-3(tm657)	3.9% (178)
psa-3(os8);unc-76;osEx[psa-3::gfp]	2.8% (176)
psa-3(os8);unc-76;osEx[mut-psa-3::gfp]	38.6% (140)
ceh-20(os39)	77.0% (122)
ceh-20(ay38)unc-36(e251)	50.0% (172)
ceh-20(os39);osEx[ceh-20::gfp]	16.1% (112)
ceh-20(os114)unc-119(e2498)	50.8% (122)
nob-1(os6)	37.7% (122)
nob-1(ct230)	35.5% (138)
*nob-1(os6);unc-76;osEx[hsp::*PSA-3*]*[a]	42.8% (112)
php-3(ok919)	12.1% (182)

[a] Results after the heat shock treatment.

blast (Berger et al., 2005). Therefore, we examined whether *nob-1* regulates the cell polarity in the T cell division. However, the asymmetric nuclear localization of POP-1 between the T cell daughters (POP-1 asymmetry) was not affected in *nob-1* mutants (normal in 26/27 *nob-1* mutants, and in 23/24 wild-type animals), indicating that *nob-1* is unlikely to be involved in cell polarity in the asymmetric T cell division.

psa-3 Encodes a Meis-Related Protein

The *psa-3* gene was genetically mapped between *unc-7* and *lin-15* on the right arm of the X chromosome (see Experimental Procedures). A cosmid, F39D8, in this region and its subclone, pPS3.11, rescued the Psa phenotype of *psa-3* mutants (Figure 2A; data not shown). In the region covered by pPS3.11, two genes are predicted in the *C. elegans* database (WormBase): *F39D8.2* and *pqn-36 (F39D8.1)*. The *pqn-36* gene is located in an intron of the *F39D8.2* gene in the inverted orientation (Figure 2A). To determine which of these predicted genes is *psa-3*, we constructed a plasmid (pPS3.16) that contained the entire *F39D8.2* gene but lacked most of the *pqn-36* gene, except its C terminus. pPS3.16 efficiently rescued the Psa phenotype of the *psa-3* mutants (Figure 2A; Table 1). To confirm that the *psa-3* gene is *F39D8.2*, we
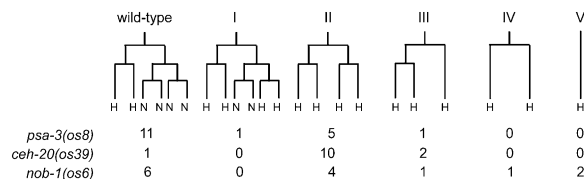

Figure 1. Abnormal T Cell Lineages in *psa-3*, *nob-1*, and *ceh-20* Mutants at the L1 Stage

H or N indicates a hypodermal or neural cell, respectively, judged by the morphology of the nucleus (Sawa et al., 2000). The numbers of T cells that showed the lineages are indicated below the diagrams.
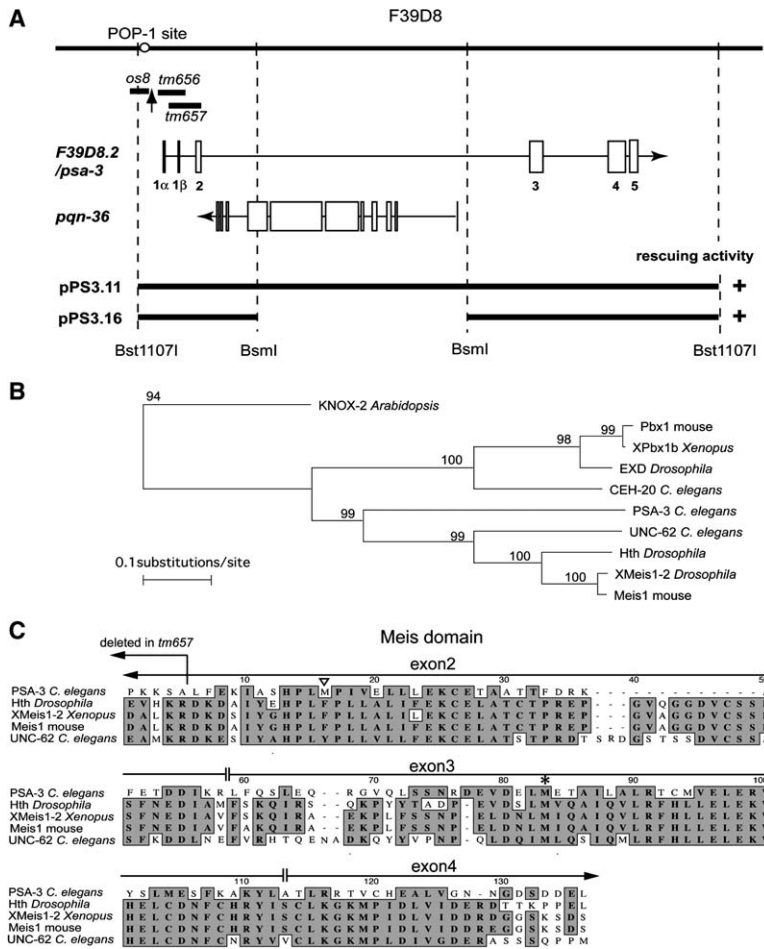
Figure 2. *psa-3* Encodes a Meis-Related Protein

(A) Schematic representation of the *psa-3* locus. Exons are indicated by open boxes. 5′ of the *F39D8.2* gene is on the left. The *pqn-36* gene is oriented inversely to the *F39D8.2* gene. The deletions in *os8*, *tm656*, and *tm657* are indicated by horizontal bars, and the point mutation in *os8* is indicated by an upward arrow. The POP-1 binding sequence is indicated by an open circle. Regions covered by the *psa-3* rescuing plasmids are indicated at the bottom.

(B) A phylogenetic tree of the Meis and PBC domains was constructed with the neighbor-joining method (Saitou and Nei, 1987) by using 153 amino acid sites. KNOX-2 in *Arabidopsis thaliana* was used as an outgroup. Bootstrap analysis was performed with 1000 replicates.

(C) Alignment of the Meis domains. An open triangle and an asterisk indicate putative initiation methionine residues from the *psa-3* transcripts that start with SL1-exon2 and SL1-exon3, respectively. The region deleted in *tm657* is indicated.

expressed a cDNA (containing exon 1β, see below) under the control of a heat shock promoter and found that the Psa phenotype of the *psa-3* mutants was efficiently rescued (Table 1). In addition, RNAi of the *F39D8.2* gene caused the Psa phenotype (Table 1). Taking these findings together, we concluded that *F39D8.2* is the *psa-3* gene.

The predicted PSA-3 protein has a domain homologous to the Meis domain (Figures 2B and 2C), but it does not have a homeobox, both of which are conserved among the previously known Meis-family transcription factors (Burglin, 1997; Mann and Affolter, 1998). By sequencing *psa-3* cDNAs, we found two alternative first exons (exon1α and exon1β). In addition, we detected transcripts in which the SL1 *trans*-spliced leader directly connected to exon2 or exon3 (Figure 2A). Of these, the SL1-exon1α and SL1-exon1β transcripts were predicted to produce proteins with an intact Meis domain. By using the first ATG in the exon as a start codon, the SL1-exon2 and SL1-exon3 transcripts were predicted to produce proteins that lacked the initial 15 amino acids and about half of the Meis domain, respectively (Figure 2C; open triangle and asterisk).

To identify the lesions in the *psa-3* gene locus, we sequenced the *psa-3* gene in the *psa-3* mutants. *os8* did not have mutations in the coding region; instead, it had a 259 bp deletion and a point mutation upstream of exon1α (Figure 2A; Experimental Procedures). The

deletion included the sequence (CTTTTGATG) to which the POP-1 protein is known to bind directly (Streit et al., 2002). PCR and Southern blot analyses indicated that *mh32* and *mh55* had DNA rearrangements in the promoter region of the *psa-3* gene (data not shown), although we did not determine the exact nature of their mutations. We also analyzed *tm656* and *tm657*, which were isolated in a PCR-based screen for deletion mutants (National BioResource Project). They had deletions in the coding region (Figure 2A; Experimental Procedures). *tm657*, but not *tm656*, exhibited the Psa phenotype, albeit weakly (Table 1). In *tm657*, all of exon1β and part of exon2 were deleted (Figures 2A and 2C), while in *tm656*, all of exon1α and exon1β were deleted, but none of exon2, which includes the region encoding the Meis domain (Figure 2A). Therefore, *tm656* probably lacked the Psa phenotype because it produced functional *psa-3* transcripts that started from SL1-exon2.

The *psa-3*/Meis Expression Is Regulated by POP-1/TCF

As described above, *psa-3(os8)* had a deletion of the putative POP-1 binding sequence, raising the possibility that *psa-3* is a target gene of POP-1. To examine this possibility, we analyzed *psa-3* expression by using a *gfp* fusion construct containing the *psa-3* promoter and the entire coding region. This construct rescued
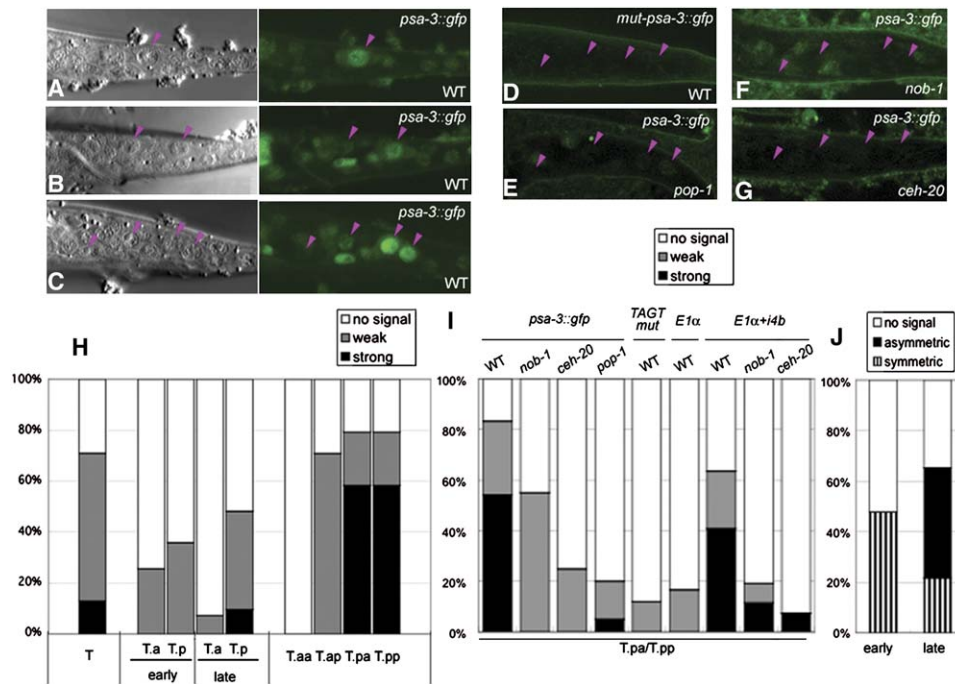
Figure 3. *psa-3* Expression Is Regulated by *pop-1*, *nob-1*, and *ceh-20*

(A–C) The expression of *psa-3::gfp* in the (A) T cell, (B) its daughters, and (C) its granddaughters in wild-type. Arrowheads indicate the nucleus of the T cell and its descendants. Anterior is to the left, and ventral is to the bottom.

(D–G) *psa-3* expression in the granddaughters of the T cell was examined, by using either (D) *mut-psa-3::gfp* with an altered POP-1 binding site in wild-type or (E) *psa-3::gfp* in *pop-1(q645)*, (F) *nob-1(os6)*, or (G) *ceh-20(os39)* mutants.

(H–J) The intensity of *psa-3::gfp* was examined in the T cell or its progeny. In each experiment, more than 20 samples were scored. "Early" and "late" indicate before and after the V6 cell division, respectively, which occurs ~30 min after the T cell division. The signal intensity representing "strong expression" (black bars) or "weak expression" (gray bars) was more or less than five times higher than background (no signal, open bars), respectively. (H) *psa-3* expression in T cells, daughter cells, or granddaughter cells in wild-type. (I) Expression of the indicated *psa-3::gfp* fusion constructs (see Figure 4A) in the posterior granddaughter cells (T.pa or T.pp) was examined in wild-type (WT), or *nob-1(os6)*, *ceh-20(os39)*, or *pop-1(q645)* mutants. (J) Animals that showed asymmetric or symmetric *psa-3* expression in the daughter cells were scored. "Asymmetric" (black bars) and "symmetric" (vertical hatched bars) mean that the intensities were higher in T.p than in T.a and equal between T.a and T.p, respectively.

the Psa phenotype of the *psa-3* mutants (Table 1). *psa-3* was expressed in the T cell, head neurons, posterior gut cells, hypodermal cells (hyp7, hyp9, and hyp10), and P blast cells (Figure 3A; data not shown). Of the seam cells, only the T cell expressed *psa-3* (data not shown). During mitosis of the T cell, the PSA-3 protein was uniformly distributed in the T cell (data not shown). Soon after the T cell division (before V6 cell division, which occurs about 30 min after T cell division), the *psa-3* expression in the two daughter cells was almost the same (Figures 3H and 3J; the early stage). In the later stage, after V6 cell division, the *psa-3* expression in T.a had decreased and that in T.p increased (Figures 3B, 3H, and 3J; the late stage). After the next round of divisions, the *psa-3* expression had greatly increased in the posterior (T.pa and T.pp), but not the anterior, granddaughters (Figures 3C and 3H). These data suggest that *psa-3* expression was induced in T.p after the T cell division, and that it accumulated in the posterior granddaughters.

To analyze the role of the putative POP-1 binding site in the promoter, we made a mutant *psa-3::gfp* construct (*mut-psa-3::gfp*) that had specific nucleotide substitutions within the POP-1 binding sequence (CTTTTGATG to CTGGAGATG; mutated nucleotides are underlined)

that were shown previously to disrupt POP-1 binding (Streit et al., 2002). We found that the *psa-3* expression and the rescuing activity were lost in the *mut-psa-3::gfp* construct (Figure 3D; Table 1). In addition, *psa-3* expression in the T.p lineage was much lower in a *pop-1* hypomorphic allele, *q645* (Figures 3E and 3I). POP-1 function is known to be required in T.p to determine the neural fate (Herman, 2001). Therefore, we concluded that POP-1 regulates *psa-3* expression in T.p through the POP-1 binding site.

We further examined the *psa-3* expression in *lin-44*/ Wnt or *lin-17*/Frizzled mutants (see Table S1 in the Supplemental Data available with this article online). In wild-type, the *psa-3* expression was higher in T.p than in T.a. in most animals in which expression was detected (T.a < T.p in Table S1). In contrast, most *lin-44* or *lin-17* mutants did not show this expression pattern, but instead showed a symmetric or reversed pattern (T.a = T.p or T.a > T.p in Table S1). The defective *psa-3* expression in *lin-44* or *lin-17* mutants was consistent with the previous observation that the cell fates of T.a and T.p are frequently reversed or symmetric in *lin-44* or *lin-17* mutants (Herman, 2002). Taking these findings together, we concluded that *psa-3* is a target gene of the Wnt signaling pathway.

NOB-1/Hox and CEH-20/Pbx Are Positive Regulators of *psa-3*/Meis Expression

After the seam cell divisions, an asymmetric nuclear localization of POP-1 (POP-1 asymmetry) is observed in all of the daughter cells (Herman, 2001; Lin et al., 1998), and the asymmetric division of all seam cells is regulated, at least, by *lit-1* and *mom-4*, which are upstream regulators of POP-1 in the Wnt-MAPK pathway (Takeshita and Sawa, 2005). Therefore, POP-1 is likely to regulate the asymmetric division of all seam cells. However, we showed that *psa-3*, a target gene of POP-1, is specifically expressed in the T cell and its descendants among the seam cells. To examine the possibility that the T cell-specific *psa-3* expression is regulated by a *Hox* gene and its cofactor, we analyzed the expression of *psa-3* in *nob-1* and *ceh-20* mutants. In these mutants, *psa-3* expression was decreased in the T.p lineage (Figures 3F, 3G, and 3I). Therefore, NOB-1 and CEH-20 function as positive regulators of *psa-3* expression. The *psa-3* expression defect in *nob-1* mutants was weaker than that in the *ceh-20* or *pop-1* mutants, suggesting that another posterior *Hox* gene, *php-3*, may function redundantly in the T cell lineage. Consistent with this, a *php-3* deletion mutant also exhibited the Psa phenotype (Table 1).

Because NOB-1 and CEH-20 are transcription factors, they are likely to regulate the transcription of *psa-3*. However, among all of the seam cells, NOB-1 and CEH-20 might bind and stabilize PSA-3 in only the T cell. To examine this possibility, we transiently expressed the PSA-3::GFP fusion protein by using a heat shock promoter, and we examined its stability in the seam cells during the L1 stage. The level of the ectopically expressed PSA-3::GFP protein decreased at a similar rate in all of the seam cells (data not shown). Therefore, this result appears to indicate that the T cell-specific PSA-3::GFP expression among seam cells is not achieved by CEH-20 and NOB-1 stabilizing the PSA-3 protein.

NOB-1/Hox and CEH-20/Pbx Directly Regulate *psa-3*/Meis Expression through Intron4

To examine how NOB-1 and CEH-20 regulate *psa-3* expression, we searched for regulatory elements in the *psa-3* gene that were required for its expression by using a series of deletion constructs of *psa-3::gfp* (Figure 4A). The deletion constructs *E1α*, *E2*, *E2-3*, and *E3* showed very weak expression, if any, in the T cell lineage, suggesting the presence of regulatory elements downstream of exon3. Deletion of intron4 (Δ*i4*), but not intron3 (Δ*i3*), also caused the loss of expression, indicating the presence of the regulatory elements in intron4. We further deleted parts of intron4 without affecting the splice sites (Δ*i4a* and Δ*i4b*). The *gfp* expression was decreased with the Δ*i4b* construct, but not with Δ*i4a*. With a smaller deletion (135 bp) in intron4 (Δ*i4c*), the *gfp* expression was also decreased, indicating that this 135 bp region (the i4c region) was essential for *psa-3* expression. To analyze the role of intron4 in more detail, we inserted the i4b region into the *E1α* construct downstream of the POP-1 binding site (*E1α+i4b*). This construct showed much stronger expression than the *E1α* construct (Figures 3I and 4A), confirming the presence of an enhancer element in the i4b region. In *nob-1* or *ceh-20* mutants carrying the *E1α+i4b* con-

struct, there was almost no *gfp* expression (Figure 3I), indicating that the element is responsible for the activity of NOB-1 and CEH-20. We concluded that NOB-1 and CEH-20 regulate *psa-3* expression though an enhancer element in intron4.

To investigate whether NOB-1/Hox and CEH-20/Pbx directly regulate *psa-3*/Meis expression, we searched for binding sequences for CEH-20 (TGA[T or A]) (Liu and Fire, 2000) within the i4c region (a consensus binding sequence for NOB-1 has not been reported). We identified two candidate sites (Figure 4B; site1 and site2) and used Electrophoretic Mobility Shift Assays (EMSAs) to examine the ability of NOB-1 to bind them by using the indicated oligonucleotides (Figure 4B). Incubation of the H/P probe, which has the canonical binding sequence for the Hox-Pbx complex (Liu and Fire, 2000), with the hexahistidine-tagged NOB-1 protein (His-NOB-1) produced a single shifted band (Figure 4C, lanes 1–3). A similar shifted band was observed with the i4c-S2 probe (Figure 4C, lane 9), but not with the i4c-S1 probe (Figure 4C, lanes 4–6). The binding of NOB-1 to i4c-S2 was disrupted weakly by a mutation in the putative CEH-20 binding site (TGAT) and strongly by one in the adjacent TAGT sequence (i4c-S2 mut II and mut III, respectively; Figure 4C, lanes 12 and 13). Furthermore, the shifted band was competed out more efficiently by the cold i4c-S2 probe than by the i4c-S2 mut III probe (Figure 4C, lanes 17–19 and 20–22). Our results indicate that the NOB-1 protein specifically binds the TAGT sequence of the i4c-S2 probe.

We next examined the effects of CEH-20/Pbx on the NOB-1-DNA complexes. We found that the addition of GST fusion CEH-20 did not produce additional (supershifted) bands, but that it significantly increased the amount of NOB-1 complexed with the H/P or i4c-S2 probes (Figure 4D, lanes 1–4, 15–18; Figure 4E). Similar effects of CEH-20 were also observed even when the Pbx binding site was mutated in the H/P probe (Figure 4D, lanes 8–11; Figure 4E), suggesting that CEH-20 promotes the complex formation between NOB-1 and DNA independent of the CEH-20 binding site. This is consistent with previous reports that Abd-B-like Hox proteins, even in the presence of Pbx proteins, do not preferentially bind DNA containing the Pbx consensus site (Shen et al., 1997), and that NOB-1 belongs to the Abd-B family (Van Auken et al., 2000). The addition of an antibody against GST to a mixture of GST fusion CEH-20, His-NOB-1, and the DNA probes did not disrupt the complex formation or produce supershifted bands, while an antibody against NOB-1 disrupted the complex formation (Figure 4D, lanes 6–7, 13–14, and 20–21). These data suggest that CEH-20 does not form a stable complex with NOB-1 and DNA, at least in this assay system. One possible mechanism is that a transient protein-protein interaction between CEH-20 and NOB-1 (see below) induces a conformational change in NOB-1 that promotes its DNA binding ability. In any case, our results indicate that CEH-20 can facilitate NOB-1's binding to intron4 of the *psa-3* gene.

To validate these results in vivo, we mutated the TAGT sequence in the *psa-3::gfp* construct as in the i4c-S2 mut III probe (Figure 4A; *TAGT mut*), and we found that the *psa-3* expression from this construct was disrupted (Figures 3I and 4A). Therefore, the NOB-1 binding
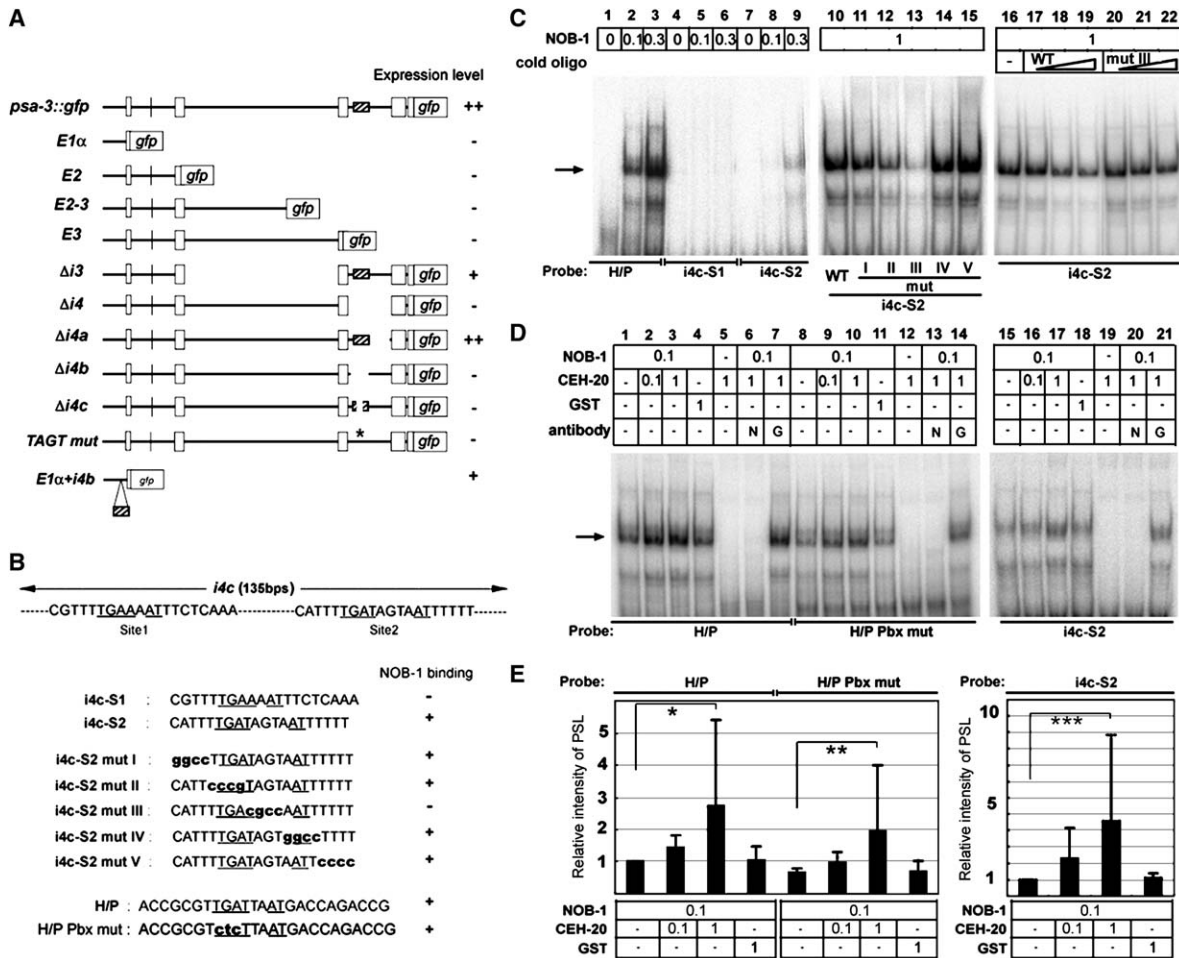
Figure 4. NOB-1 and CEH-20 Regulate *psa-3* Expression through Intron4

(A) Schematic structures of the deletion constructs of *psa-3::gfp* and their relative level of expression in the T cell granddaughters. ++ indicates that >50% of the animals showed "strong expression" (more than five times higher than background, or "no expression"). + indicates that 10%–50% of the animals showed "strong expression". − indicates no expression or "weak expression" (less than five times higher than "no expression"). Open boxes indicate the coding regions, and the hatched box indicates the i4b region (440 bps). The asterisk indicates the mutation in the NOB-1 binding sequence (TAGT to CGCC).

(B) Summary of the EMSAs and sequences of the probes that were used in them. + or − represent the presence or absence, respectively, of NOB-1 binding. The i4c-S1 or i4c-S2 probes covered site1 or site2 of the I4c region, respectively. Underlined bases indicate the putative binding sequences for CEH-20 (TGA[T or A]). i4c-S2 mut I–V were derived from i4c-S2; mutated residues are shown by bold lower-case letters. The H/P probe contains a canonical Pbx/Hox sequence including TGAT, to which CEH-20 binds, and the H/P Pbx mut probe has mutations in the TGAT sequence.

(C and D) EMSA results. The horizontal arrows indicate shifted bands corresponding to complexes of the NOB-1 proteins and probes. The amounts of the indicated proteins (shown in micrograms), cold oligonucletides, or antibodies (N, NOB-1 antibody; G, GST antibody) were co-incubated with the indicated probes. WT indicates wild-type i4c-S2 oligonucleotide.

(E) Relative amount of the protein-DNA complex estimated by photo-stimulated luminescence (PSL) by using the BAS2500 system (FUJIFILM). The PSL values were normalized to the control (coincubation of the probe and NOB-1 alone). The means and standard deviations of the relative PSL values obtained in at least three independent experiments were shown. Coincubation with CEH-20 significantly increased the intensities of the shifted bands (*p = 0.01, **p < 0.01, ***p = 0.03 in paired Student's t tests).

sequence is essential for *psa-3* expression in vivo. Taking these data together, we concluded that NOB-1 and CEH-20 directly regulate *psa-3* transcription though intron4.

psa-3/Meis Is Required for the Nuclear Localization of CEH-20/Pbx

We examined *ceh-20* expression by using a *gfp* fusion construct containing the *ceh-20* promoter and the entire coding region. This construct rescued Psa, Unc, and the larval lethal phenotype of *ceh-20* mutants (Table 1). At

the L1 stage, *ceh-20* was expressed in nearly all of the cells, including the T cell (Figure 5A; data not shown). During T cell mitosis, CEH-20 was distributed uniformly (data not shown). Soon after T cell division (before V6 division), the nuclear level of CEH-20 was equal in the daughter cells (Figure 5E; early stage in wild-type), while in the late stage, after V6 division, the nuclear level in T.a was slightly greater and that in T.p was slightly less (Figure 5E; late stage in wild-type), resulting in the differential subcellular localization of CEH-20 between the daughter cells (8/33 animals showed the asymmetric
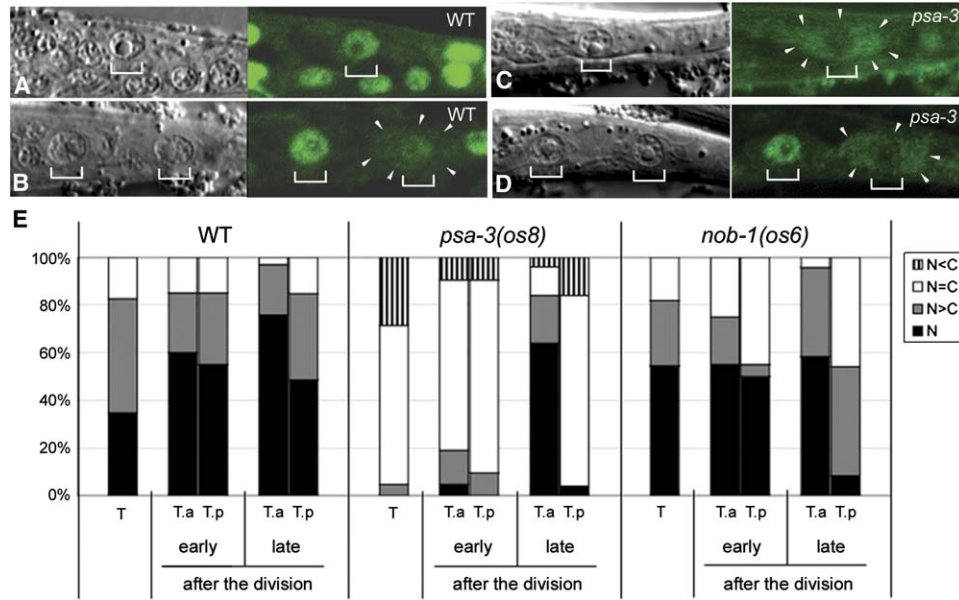
Figure 5. Nuclear Localization of CEH-20 Is Regulated by *psa-3*

(A–D) Expression of *ceh-20::gfp* in the (A) T cell and (B) its daughter cells in wild-type, or in the (C) T cell and (D) its daughter cells in *psa-3(os8)* mutants. White brackets indicate the nucleus of the T cell and its daughters. Arrowheads indicate cell boundaries visualized by the cytoplasmic CEH-20 signal. Anterior is to the left, and ventral is to the bottom.

(E) The subcellular localization of CEH-20 was examined in wild-type, *psa-3(os8)*, or *nob-1(os6)* and was classified into four types: "N" (black bars), "N > C" (gray bars), "N = C" (open bars), and "N < C" (vertical, hatched bars). "N" indicates that CEH-20 exclusively localized to the nucleus. "N > C", "N < C", and "N = C" indicate a difference between the nuclear (N) and cytoplasmic (C) signals. "Early" and "late" indicate before and after the V6 cell division, respectively. In each experiment, more than 20 samples were scored.

localization as shown in Figure 5B; i.e., strong nuclear localization in T.a and weak nuclear and cytoplasmic localization in T.p). These results suggest that the subcellular localization of CEH-20 protein is differentially regulated between the T cell daughters. To investigate the mechanism for the asymmetric nuclear localization, we examined the localization of CEH-20 protein in *psa-3* and *nob-1* mutants. In *psa-3* mutants, the nuclear localization of CEH-20 in the T cell was disrupted (Figures 5C and 5E in *psa-3(os8)* mutants). Soon after the division, the nuclear localization in both daughters was disrupted; however, at the late stage, the nuclear localization of CEH-20 in T.a was normal, but that in T.p was still disrupted (Figure 5E). At this stage, 3/25 animals showed nuclear localization in T.a and preferential cytoplasmic localization in T.p (Figure 5D). This phenotype was not observed in wild-type. Taken together, these data indicate that in both daughters soon after T cell division as well as in the T cell, CEH-20 nuclear localization is regulated by *psa-3*, while at the late stage, CEH-20 nuclear localization in T.p, but not T.a, depends on *psa-3* function. The nuclear localization of CEH-20 in T.a might be regulated by other genes, for example, by another Meis protein, UNC-62 (see Discussion). In *nob-1* mutants, as seen in *psa-3* mutants, the nuclear localization of CEH-20 in T.p was disrupted, albeit partially, in the late stage after division (Figure 5E). This result is consistent with a decreased expression of *psa-3* in the *nob-1* mutants (Figures 3F and 3I).

PSA-3/Meis Functions as a Cell Fate Determinant
The asymmetric expression of *psa-3* between T cell daughters seemed to indicate that PSA-3 functions as

a cell fate determinant in T.p (Figures 3B, 3C, and 3H). To test this possibility, we expressed *psa-3* during or just after the T cell division by using a heat shock promoter, and we found that the Psa phenotype of *psa-3* mutants was rescued, albeit partially (Figure 6A). The partial rescue might be because of the lag time between the start of the heat shock treatment and the expression of the PSA-3 protein or because PSA-3 has functions before as well as after the division. In any case, the results suggest that *psa-3* functions in T.p as a cell fate determinant.

In other organisms, Meis family proteins function as cofactors of Pbx and Hox family proteins (Mann and Affolter, 1998). We tested whether PSA-3 can interact physically with CEH-20/Pbx or NOB-1/Hox, as is observed for the Meis proteins in other organisms. We found that GST fusion PSA-3 bound specifically to in vitro-translated CEH-20 (Figure 6B). GST fusion NOB-1 also bound specifically to CEH-20 (Figure 6C). We did not detect significant direct binding between PSA-3 and NOB-1 (Figures 6B and 6C). These results are consistent with the notion that PSA-3 functions as a cofactor for the CEH-20-NOB-1 complex through its binding to CEH-20. Therefore, NOB-1 and CEH-20 not only activate *psa-3* transcription, but may also function with PSA-3 in the cell fate decision. To test this model further, we expressed *psa-3* by using a heat shock promoter in *nob-1* mutants. If *nob-1* was required only for the *psa-3* expression, the expression of *psa-3* should rescue the Psa phenotype of *nob-1* mutants. However, the ectopic expression of *psa-3* rescued the Psa phenotype of *psa-3* mutants, but not that of *nob-1* mutants (Table 1). These results suggested that, even in the presence of PSA-3,
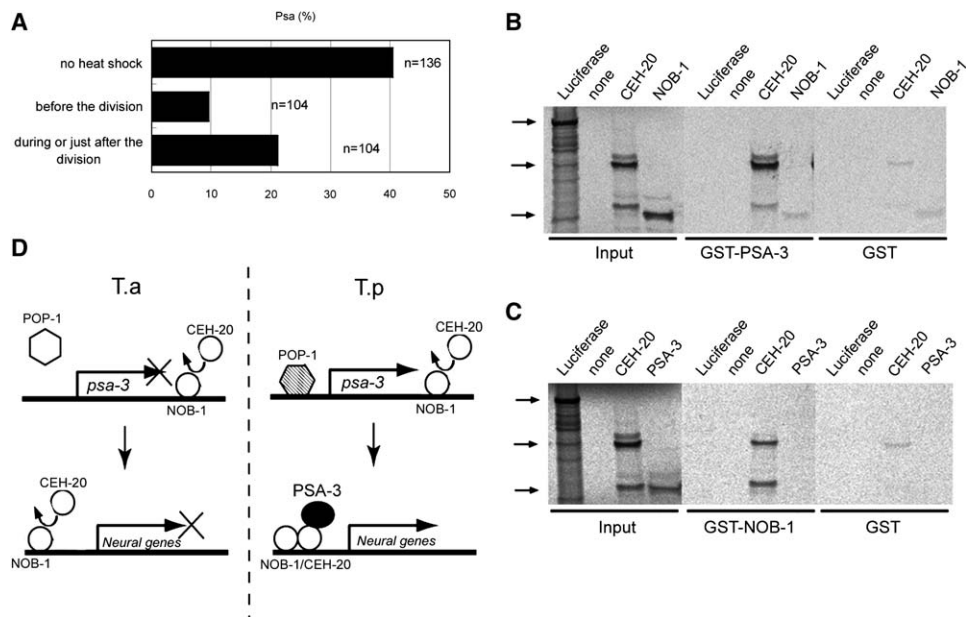
Figure 6. PSA-3 Functions as a Cell Fate Determinant, Probably with CEH-20 and NOB-1

(A) *psa-3* can function after the T cell division. Animals containing *hsp*::PSA-3, whose T cells both on the left and right sides were in mitosis or had just undergone division (as judged by morphology of the nucleus under Nomarski optics), were collected and treated with 1 hr of heat shock at 33°C (during or just after division) or further incubated at 22.5°C as a control (no heat shock). For the "before the division" experiments, the heat shock treatment was started 1 hr after hatching. The heat shock treatment "before the division" and "during or just after the division" significantly rescued the Psa phenotype ($p < 0.0001$ and $p = 0.002$ versus "no heat shock", respectively, by Fisher's exact test).

(B and C) In vitro binding assays were performed by using in vitro-translated proteins labeled with [^{35}S]methionine. The arrows indicate in vitro-translated proteins. In the "Input" lanes, we loaded 1/10 of the in vitro-translated protein that we used in the binding assays. The binding assays were performed with (A) GST fusion PSA-3 protein or (B) GST fusion NOB-1 protein. Luciferase or GST proteins were used as negative controls.

(D) A model for the asymmetric T cell division. Asymmetric T cell division results in the activation of POP-1 (hatched hexagon) in T.p; activated POP-1 binds to the *psa-3* promoter. *psa-3* is selectively induced in T.p by POP-1, and this induction requires the binding of NOB-1 to the *psa-3* intronic region, which is promoted by CEH-20. After its induction, PSA-3 forms a complex with NOB-1 and CEH-20, and this complex functions as a cell fate determinant in T.p to induce genes required for the neural fates of its progeny in the tail region. In T.a, PSA-3 is not induced because POP-1 is not active.

NOB-1 function is required for cell fate determination. Taken together, these results support a model in which the PSA-3 protein functions as a cofactor of NOB-1 and CEH-20 to regulate the cell fate of T.p after the asymmetric T cell division (Figure 6D).

Discussion

In this study, we showed that *psa-3*/Meis expression is regulated by POP-1/TCF, as well as by NOB-1/Hox and CEH-20/Pbx. We also showed that *psa-3* can function after the T cell division as a cell fate determinant. POP-1 is a universal factor that determines asymmetry between daughter cells (Herman, 2001; Lin et al., 1998), while NOB-1 regulates the positional identity of cells (Van Auken et al., 2000). Therefore, we conclude that the specific fate of T.p is determined by the cooperation of genes that regulate asymmetric cell division and positional identity, through the induction of *psa-3*/Meis.

Mechanisms for *psa-3*/Meis Expression and CEH-20/Pbx Nuclear Localization

In wild-type animals, PSA-3 is expressed before the T cell division, and PSA-3 proteins are inherited equally by the T cell daughters. At the early stage after T cell division, when it is expressed equally in both daughters, PSA-3 is likely to function in the nuclear localization of CEH-20 in both daughter cells. In T.p, nuclear CEH-20 promotes the DNA binding ability of NOB-1, which activates *psa-3* transcription in cooperation with POP-1 (Figure 6D). In the late stage after T cell division, when *psa-3* expression is induced in T.p, PSA-3 functions to maintain CEH-20's nuclear localization in T.p, while in T.a, CEH-20's nuclear localization does not appear to depend on *psa-3* function, because in *psa-3* mutants, CEH-20 protein was accumulated normally in the T.a nucleus at the late stage of T cell division (Figures 5D and 5E). In other organisms, the subcellular localization of Pbx family proteins is regulated by their binding with Meis family proteins as well as by phosphorylation by PKC or by direct binding with nonmuscle Myosin (Affolter et al., 1999; Huang et al., 2003; Kilstrup-Nielsen et al., 2003). Similar mechanisms may be used for the nuclear localization of CEH-20 in T.a in *C. elegans*. Because the CEH-20 nuclear localization is disrupted in T.p, but not in T.a in *psa-3* mutants, such *psa-3*-independent mechanisms are likely to operate only in T.a and hence may be under the control of the Wnt-MAPK pathway.

PSA-3/Meis May Function as a Non-DNA Binding Activator of the CEH-20-Pbx-NOB-1-Hox Complex

Among the Meis family proteins, PSA-3 is unique because it lacks a homeobox. In other organisms, the

requirement of a homeobox for Meis protein function remains controversial. Mutant Meis proteins (Meis1.1 in zebrafish or Homothorax in *Drosophila*) that lack the homeobox act as dominant-negative forms (Ryoo et al., 1999; Waskiewicz et al., 2001). In contrast, mutant Meis3 proteins lacking a homeobox in zebrafish and *Xenopus* do not show dominant-negative effects and can even activate Pbx-Hox-dependent transcription in vivo (Choe et al., 2002; Salzberg et al., 1999). In addition, mutant Meis proteins (Meis1A or Prep1) that do not bind DNA can enhance the DNA binding activity of the Hox-Pbx complex in vitro (Berthelsen et al., 1998; Shanmugam et al., 1999). In *Drosophila*, deletion of the homeobox in the *homothorax* gene causes only partial and weak defects in the peripheral nervous system, whereas mutations affecting the Meis domain cause much more severe phenotypes. Given these observations, it was proposed that the homeobox-less Homothorax retains some of its transcription-regulating function via its interaction with Extradenticle/Pbx (Kurant et al., 2001). In our study, loss-of-function mutants of *psa-3*, *ceh-20*, or *nob-1* had the same defect in the asymmetric T cell division. Therefore, although PSA-3 lacks a homeobox, it is likely that it positively regulates CEH-20 and NOB-1 rather than inhibiting them by acting as a dominant-negative form. For example, although CEH-20 did not stably bind to DNA with NOB-1, at least in our EMSA experiments, PSA-3 may stabilize their interaction. In this model, PSA-3 induced in a T.p cell stabilizes the CEH-20-NOB-1 complex on DNA, while in a T.a cell, CEH-20 cannot stably interact with DNA (Figure 6D). Further analyses are necessary to clarify the roles of PSA-3 in cell fate determination.

Do *Hox* Genes Regulate Asymmetric Cell Division in Vertebrates?

In this study, we showed that cooperation between the mechanisms for asymmetric cell division and positional identity determines the specific cell fate in asymmetric T cell division in *C. elegans*. Such cooperation may explain how the general mechanism for asymmetric division specifies individual cell fates in other organisms. In vertebrates, *Hox* genes play essential roles in the development of the segmental pattern of the central nervous system. They also regulate the segmental identities of specific neurons. In the hindbrain, *Hox* genes are involved in the fate determination of specific motor neurons, such as branchial and somatic motoneurons and sensory interneurons, like the visceral and somatic sensory interneurons (Gaufo et al., 2003, 2004; Samad et al., 2004). In the spinal cord, the identities of the unique motor neurons in individual segmental domains are determined by *Hox* genes (Dasen et al., 2003). During neurogenesis, neurons are generated through the asymmetric divisions of neuroepithelial cells or neuronal progenitor cells (Chenn and McConnell, 1995; Kosodo et al., 2004). Therefore, it is possible that *Hox* genes regulate the segmental specificities of neurons when they are generated by asymmetric cell divisions in vertebrate neurogenesis.

Similarly, some Hox, Pbx, and Meis proteins are expressed and function in hematopoietic stem cells (HSCs) and in specific hematopoietic cell lineages (DiMartino et al., 2001; Hisa et al., 2004; Pineault et al., 2002). Although it remains to be proved, some studies have suggested that HSCs undergo asymmetric cell division (Denkers et al., 1993; Ema et al., 2000; Ho, 2005; Takano et al., 2004). Thus, Hox proteins and their cofactors may specify hematopoietic lineages upon asymmetric cell division in a manner that is similar to the one we have described here for the T cell in *C. elegans*.

Experimental Procedures

Genetic Experiments
Methods for the culture and genetic manipulation of *C. elegans* were as described (Brenner, 1974; Sawa et al., 2000). The Psa phenotype was determined as described (Sawa et al., 2000). Fluorescence from GFP fusion proteins was observed with a confocal microscope (LSM510 system by Carl Zeiss), and the intensity of the GFP fluorescence was measured by the system's software. RNAi assays for *psa-3* were carried out by microinjecting double-stranded RNAs synthesized by using part of exon4 (∼200 bp fragment of yk375g3) (Fire et al., 1998). To map *psa-3*, we isolated recombinants from *unc-7 lin-15/psa-3(os8)*. Five of 14 Unc non-Lin recombinants segregated with *psa-3*. Seven of ten Lin non-Unc recombinants segregated with *psa-3*. The deletion in *psa-3(os8)* was located between −514 and −256 bps, and the point mutation was at −185 bp upstream of the initiation codon in exon1α. The deletions in *tm656* and *tm657* are described in the National BioResource Project (http://www.nbrp.jp/report/reportProject.jsp?project=celegans).

Plasmid Construction
A 14 kb Bst1107I fragment of F39D8 was subcloned into pBSK to produce pPS3.11. A 5 kb BsmI fragment containing the *pqn-36* gene was removed from pPS3.11 to generate pPS3.16. To generate *psa-3::gfp*, the entire *psa-3* coding region within pPS3.16 was subcloned into a GFP vector, pPD95.77 (a gift from Dr. A. Fire, Stanford University, Stanford, CA), after removal of the 3′ UTR region containing the stop codon. *mut-psa-3::gfp*, shown in Figure 3D, and *Δ4* to *TAGT mut*, shown in Figure 4A, were made by a PCR-based method, and their sequences were confirmed by direct sequencing. *hsp::PSA-3* and *hsp::PSA-3::gfp* were constructed by subcloning the *psa-3* cDNA or the *gfp* fusion *psa-3* cDNA, respectively, whose product was GFP joined to the C terminus of PSA-3, into pPD49.78 (a gift from Dr. A. Fire). For the heat shock experiments, animals were incubated at 33ºC for 1 hr and overnight at 22.5ºC. *ceh-20::gfp* was constructed by inserting a *gfp* fragment from pPD118.90 (a gift from Dr. A. Fire) into a PstI site in exon4 of the *ceh-20* gene (the rescuing plasmid was a gift from Dr. M. Stern, Yale University, New Haven, CT).

In Vitro Binding Assay and EMSA
For the GST fusion proteins or hexahistidine-tagged proteins, the cDNAs of *psa-3*, *ceh-20*, and *nob-1* in yk375g3, yk219d9, and yk467d4, respectively, were subcloned into pGex6P or pQE-82L (Amersham and QIAGEN). yk219d9 was used after removal of the 5′ region, as described (Liu and Fire, 2000). Purification of proteins expressed in *E. coli* (BL-21) and in vitro binding assays was performed as described (Tomoda et al., 1999). ^{35}S-labeled proteins were synthesized by the TNT T7/T3-coupled Reticulocyte Lysate System (Promega). EMSAs were performed by using probes labeled with α-^{32}P-dCTP by the Klenow fragment (Asubel et al., 1996). Rabbit antibody against NOB-1 was produced by using GST fusion NOB-1 protein.

Supplemental Data
Supplemental Data include one table and are available at http://www.developmentalcell.com/cgi/content/full/11/1/105/DC1/.

References

Affolter, M., Marty, T., and Vigano, M.A. (1999). Balancing import and export in development. Genes Dev. *13*, 913–915.

Asubel, F.M., Brent, R., Kingston, R.E., Moore, D.D., Seidman, J.G., Smith, J.A., and Struhl, K. (1996). Current Protocols in Molecular Biology, Volume 2 (New York: John Wiley and Sons, Inc.).

Berger, C., Pallavi, S.K., Prasad, M., Shashidhara, L.S., and Technau, G.M. (2005). A critical role for *cyclin E* in cell fate determination in the central nervous system of *Drosophila melanogaster*. Nat. Cell Biol. *7*, 56–62.

Berthelsen, J., Zappavigna, V., Ferretti, E., Mavilio, F., and Blasi, F. (1998). The novel homeoprotein Prep1 modulates Pbx-Hox protein cooperativity. EMBO J. *17*, 1434–1445.

Bhat, K.M. (1999). Segment polarity genes in neuroblast formation and identity specification during *Drosophila* neurogenesis. Bioessays *21*, 472–485.

Brenner, S. (1974). The genetics of *Caenorhabditis elegans*. Genetics *77*, 71–94.

Burglin, T.R. (1997). Analysis of TALE superclass homeobox genes (MEIS, PBC, KNOX, Iroquois, TGIF) reveals a novel domain conserved between plants and animals. Nucleic Acids Res. *25*, 4173–4180.

Chenn, A., and McConnell, S.K. (1995). Cleavage orientation and the asymmetric inheritance of Notch1 immunoreactivity in mammalian neurogenesis. Cell *82*, 631–641.

Choe, S.K., Vlachakis, N., and Sagerstrom, C.G. (2002). Meis family proteins are required for hindbrain development in the zebrafish. Development *129*, 585–595.

Dasen, J.S., Liu, J.P., and Jessell, T.M. (2003). Motor neuron columnar fate imposed by sequential phases of Hox-c activity. Nature *425*, 926–933.

Denkers, I.A., Dragowska, W., Jaggi, B., Palcic, B., and Lansdorp, P.M. (1993). Time lapse video recordings of highly purified human hematopoietic progenitor cells in culture. Stem Cells *11*, 243–248.

DiMartino, J.F., Selleri, L., Traver, D., Firpo, M.T., Rhee, J., Warnke, R., O'Gorman, S., Weissman, I.L., and Cleary, M.L. (2001). The Hox cofactor and proto-oncogene Pbx1 is required for maintenance of definitive hematopoiesis in the fetal liver. Blood *98*, 618–626.

Ema, H., Takano, H., Sudo, K., and Nakauchi, H. (2000). *In vitro* self-renewal division of hematopoietic stem cells. J. Exp. Med. *192*, 1281–1288.

Fire, A., Xu, S., Montgomery, M.K., Kostas, S.A., Driver, S.E., and Mello, C.C. (1998). Potent and specific genetic interference by double-stranded RNA in *Caenorhabditis elegans*. Nature *391*, 806–811.

Gaufo, G.O., Thomas, K.R., and Capecchi, M.R. (2003). *Hox3* genes coordinate mechanisms of genetic suppression and activation in the generation of branchial and somatic motoneurons. Development *130*, 5191–5201.

Gaufo, G.O., Wu, S., and Capecchi, M.R. (2004). Contribution of *Hox* genes to the diversity of the hindbrain sensory system. Development *131*, 1259–1266.

Herman, M. (2001). *C. elegans* POP-1/TCF functions in a canonical Wnt pathway that controls cell migration and in a noncanonical Wnt pathway that controls cell polarity. Development *128*, 581–590.

Herman, M.A. (2002). Control of cell polarity by noncanonical Wnt signaling in *C. elegans*. Semin. Cell Dev. Biol. *13*, 233–241.

Hisa, T., Spence, S.E., Rachel, R.A., Fujita, M., Nakamura, T., Ward, J.M., Devor-Henneman, D.E., Saiki, Y., Kutsuna, H., Tessarollo, L., et al. (2004). Hematopoietic, angiogenic and eye defects in Meis1 mutant animals. EMBO J. *23*, 450–459.

Ho, A.D. (2005). Kinetics and symmetry of divisions of hematopoietic stem cells. Exp. Hematol. *33*, 1–8.

Huang, H., Paliouras, M., Rambaldi, I., Lasko, P., and Featherstone, M. (2003). Nonmuscle myosin promotes cytoplasmic localization of PBX. Mol. Cell. Biol. *23*, 3636–3645.

Jan, Y.N., and Jan, L.Y. (2001). Asymmetric cell division in the *Drosophila* nervous system. Nat. Rev. Neurosci. *2*, 772–779.

Kaletta, T., Schnabel, H., and Schnabel, R. (1997). Binary specification of the embryonic lineage in *Caenorhabditis elegans*. Nature *390*, 294–298.

Kenyon, C.J., Austin, J., Costa, M., Cowing, D.W., Harris, J.M., Honigberg, L., Hunter, C.P., Maloof, J.N., Muller-Immergluck, M.M., Salser, S.J., et al. (1997). The dance of the *Hox* genes: patterning the anteroposterior body axis of *Caenorhabditis elegans*. Cold Spring Harb. Symp. Quant. Biol. *62*, 293–305.

Kidd, A.R., 3rd, Miskowski, J.A., Siegfried, K.R., Sawa, H., and Kimble, J. (2005). A beta-catenin identified by functional rather than sequence criteria and its role in Wnt/MAPK signaling. Cell *121*, 761–772.

Kilstrup-Nielsen, C., Alessio, M., and Zappavigna, V. (2003). PBX1 nuclear export is regulated independently of PBX-MEINOX interaction by PKA phosphorylation of the PBC-B domain. EMBO J. *22*, 89–99.

Koh, K., Peyrot, S.M., Wood, C.G., Wagmaister, J.A., Maduro, M.F., Eisenmann, D.M., and Rothman, J.H. (2002). Cell fates and fusion in the *C. elegans* vulval primordium are regulated by the EGL-18 and ELT-6 GATA factors–apparent direct targets of the LIN-39 Hox protein. Development *129*, 5171–5180.

Kosodo, Y., Roper, K., Haubensak, W., Marzesco, A.M., Corbeil, D., and Huttner, W.B. (2004). Asymmetric distribution of the apical plasma membrane during neurogenic divisions of mammalian neuroepithelial cells. EMBO J. *23*, 2314–2324.

Kurant, E., Eytan, D., and Salzberg, A. (2001). Mutational analysis of the *Drosophila* homothorax gene. Genetics *157*, 689–698.

Lin, R., Hill, R.J., and Priess, J.R. (1998). POP-1 and anterior-posterior fate decisions in *C. elegans* embryos. Cell *92*, 229–239.

Liu, J., and Fire, A. (2000). Overlapping roles of two Hox genes and the exd ortholog *ceh-20* in diversification of the *C. elegans* postembryonic mesoderm. Development *127*, 5179–5190.

Mann, R.S., and Affolter, M. (1998). Hox proteins meet more partners. Curr. Opin. Genet. Dev. *8*, 423–429.

Pineault, N., Helgason, C.D., Lawrence, H.J., and Humphries, R.K. (2002). Differential expression of *Hox*, *Meis1*, and *Pbx1* genes in primitive cells throughout murine hematopoietic ontogeny. Exp. Hematol. *30*, 49–57.

Ryoo, H.D., Marty, T., Casares, F., Affolter, M., and Mann, R.S. (1999). Regulation of Hox target genes by a DNA bound Homothorax/Hox/Extradenticle complex. Development *126*, 5137–5148.

Saitou, N., and Nei, M. (1987). The neighbor-joining method: a new method for reconstructing phylogenetic trees. Mol. Biol. Evol. *4*, 406–425.

Salser, S.J., and Kenyon, C. (1996). A *C. elegans* Hox gene switches on, off, on and off again to regulate proliferation, differentiation and morphogenesis. Development *122*, 1651–1661.

Salzberg, A., Elias, S., Nachaliel, N., Bonstein, L., Henig, C., and Frank, D. (1999). A Meis family protein caudalizes neural cell fates in *Xenopus*. Mech. Dev. *80*, 3–13.

Samad, O.A., Geisen, M.J., Caronia, G., Varlet, I., Zappavigna, V., Ericson, J., Goridis, C., and Rijli, F.M. (2004). Integration of anteroposterior and dorsoventral regulation of Phox2b transcription in cranial motoneuron progenitors by homeodomain proteins. Development *131*, 4071–4083.

Sawa, H., Kouike, H., and Okano, H. (2000). Components of the SWI/SNF complex are required for asymmetric cell division in *C. elegans*. Mol. Cell *6*, 617–624.

Shanmugam, K., Green, N.C., Rambaldi, I., Saragovi, H.U., and Featherstone, M.S. (1999). PBX and MEIS as non-DNA-binding partners in trimeric complexes with HOX proteins. Mol. Cell. Biol. *19*, 7577–7588.

Shen, W.F., Rozenfeld, S., Lawrence, H.J., and Largman, C. (1997). The Abd-B-like Hox homeodomain proteins can be subdivided by the ability to form complexes with Pbx1a on a novel DNA target. J. Biol. Chem. *272*, 8198–8206.

Shetty, P., Lo, M.C., Robertson, S.M., and Lin, R. (2005). *C. elegans* TCF protein, POP-1, converts from repressor to activator as a result of Wnt-induced lowering of nuclear levels. Dev. Biol. *285*, 584–592.

Streit, A., Kohler, R., Marty, T., Belfiore, M., Takacs-Vellai, K., Vigano, M.A., Schnabel, R., Affolter, M., and Muller, F. (2002). Conserved regulation of the *Caenorhabditis elegans* labial/Hox1 gene *ceh-13*. Dev. Biol. *242*, 96–108.

Takano, H., Ema, H., Sudo, K., and Nakauchi, H. (2004). Asymmetric division and lineage commitment at the level of hematopoietic stem cells: inference from differentiation in daughter cell and granddaughter cell pairs. J. Exp. Med. *199*, 295–302.

Takeshita, H., and Sawa, H. (2005). Asymmetric cortical and nuclear localizations of WRM-1/beta-catenin during asymmetric cell division in *C. elegans*. Genes Dev. *19*, 1743–1748.

Thorpe, C.J., Schlesinger, A., and Bowerman, B. (2000). Wnt signalling in *Caenorhabditis elegans*: regulating repressors and polarizing the cytoskeleton. Trends Cell Biol. *10*, 10–17.

Tomoda, K., Kubota, Y., and Kato, J. (1999). Degradation of the cyclin-dependent-kinase inhibitor p27Kip1 is instigated by Jab1. Nature *398*, 160–165.

Van Auken, K., Weaver, D.C., Edgar, L.G., and Wood, W.B. (2000). *Caenorhabditis elegans* embryonic axial patterning requires two recently discovered posterior-group *Hox* genes. Proc. Natl. Acad. Sci. USA *97*, 4499–4503.

Van Auken, K., Weaver, D., Robertson, B., Sundaram, M., Saldi, T., Edgar, L., Elling, U., Lee, M., Boese, Q., and Wood, W.B. (2002). Roles of the Homothorax/Meis/Prep homolog UNC-62 and the Exd/Pbx homologs CEH-20 and CEH-40 in *C. elegans* embryogenesis. Development *129*, 5255–5268.

Waskiewicz, A.J., Rikhof, H.A., Hernandez, R.E., and Moens, C.B. (2001). Zebrafish Meis functions to stabilize Pbx proteins and regulate hindbrain patterning. Development *128*, 4139–4151.

Zhao, X., Yang, Y., Fitch, D.H., and Herman, M.A. (2002). TLP-1 is an asymmetric cell fate determinant that responds to Wnt signals and controls male tail tip morphogenesis in *C. elegans*. Development *129*, 1497–1508.

Accession Numbers

The NCBI accession number for the *psa-3* sequence reported in this paper is DQ118141.